The effect of relative humidity on eddy covariance latent heat flux measurements and its implication for partitioning into transpiration and evaporation

Weijie Zhang [a,b,*], Martin Jung [a], Mirco Migliavacca [a,c], Rafael Poyatos [d,e], Diego G. Miralles [b], Tarek S. El-Madany [a], Marta Galvagno [f], Arnaud Carrara [g], Nicola Arriga [c], Andreas Ibrom [h], Ivan Mammarella [i], Dario Papale [j,k], Jamie R. Cleverly [l], Michael Liddell [l], Georg Wohlfahrt [m], Christian Markwitz [n], Matthias Mauder [o], Eugenie Paul-Limoges [p], Marius Schmidt [q], Sebastian Wolf [r], Christian Brümmer [s], M. Altaf Arain [t], Silvano Fares [u], Tomomichi Kato [v], Jonas Ardö [w], Walter Oechel [x,y], Chad Hanson [z], Mika Korkiakoski [i], Sébastien Biraud [aa], Rainer Steinbrecher [ab], Dave Billesbach [ac], Leonardo Montagnani [ad], William Woodgate [ae,af], Changliang Shao [ag], Nuno Carvalhais [a,ah], Markus Reichstein [a,ai], Jacob A. Nelson [a]

[a] Department of Biogeochemical Integration, Max Planck Institute for Biogeochemistry, Jena, Germany
[b] Hydro-Climate Extremes Lab (H-CEL), Faculty of Bioscience Engineering, Ghent University, Ghent, Belgium
[c] European Commission, Joint Research Centre, Ispra, (VA), Italy
[d] CREAF, Cerdanyola del Vallès, Spain
[e] Universitat Autònoma de Barcelona, Cerdanyola del Vallès, Spain
[f] Climate Change Unit, Environmental Protection Agency of Aosta Valley, Aosta, Italy
[g] Fundación Centro de Estudios Ambientales del Mediterráneo, 46980, Paterna, Valencia, Spain
[h] Technical University of Denmark, Department of Environment and Resource Management, Kgs, Lyngby, Denmark
[i] Institute for Atmospheric and Earth System Research/Physics (INAR), Faculty of Science, P.O. Box 68, 00014 University of Helsinki, Helsinki, Finland
[j] University of Tuscia - DIBAF, 01100, Viterbo, Italy
[k] euroMediterranean Center on Climate Change (CMCC) - IAFES, 01100, Viterbo, Italy
[l] College of Science and Engineering, James Cook University, Cairns, QLD, 4878, Australia
[m] Department of Ecology, University of Innsbruck, Innsbruck, Austria
[n] Bioclimatology, University of Göttingen, Göttingen, Germany
[o] Technische Universität Dresden, Faculty of Environmental Sciences, Dresden, Germany
[p] Department of Geography, University of Zurich, 8057, Zurich, Switzerland
[q] Agrosphere Institute, IBG-3, Forschungszentrum Jülich GmbH, 52425, Jülich, Germany
[r] Department of Environmental Systems Science, ETH Zurich, 8092, Zurich, Switzerland
[s] Thünen Institute of Climate-Smart Agriculture, Braunschweig, Germany
[t] School of Earth, Environment and Society, McMaster University, Hamilton, Ontario, Canada
[u] National Research Council of Italy, Institute of Bioeconomy, Rome, Italy
[v] Research Faculty of Agriculture, Hokkaido University, Sapporo, Japan
[w] Department of Physical Geography and Ecosystem Science, Lund University, Sweden
[x] Global Change Research Group, San Diego State University, San Diego, CA, USA
[y] Department of Geography, University of Exeter, Exeter, UK
[z] Department of Forests Ecosystems and Society, College of Forestry, Oregon State University, Corvallis, OR, USA
[aa] Climate Sciences Department, Lawrence Berkeley National Laboratory, Berkeley, CA, USA
[ab] Karlsruhe Institute of Technology (KIT), Institute of Meteorology and Climate Research (IMK), DepartmentAtmospheric Environmental Research (IFU), Garmisch-Partenkirchen, Germany
[ac] University of Nebraska, Lincoln, NE, USA
[ad] Faculty of Science and Technology, Free University of Bozen-Bolzano, 39100, Bolzano, Italy
[ae] School of Earth and Environmental Sciences, The University of Queensland, Saint Lucia, 4072, QLD, Australia
[af] Space and Astronomy, CSIRO, Kensington, 6151, Australia
[ag] Institute of Agricultural Resources and Regional Planning, Chinese Academy of Agricultural Sciences, Beijing, China
[ah] Departamento de Ciências e Engenharia do Ambiente (DCEA), Faculdade de Ciências e Tecnologia (FCT), Universidade Nova de Lisboa, Lisbon, Portugal
[ai] Michael-Stifel-Center Jena for Data-Driven and Simulation Science, Jena, Germany

* Corresponding author.
E-mail address: wzhang@bgc-jena.mpg.de (W. Zhang).

A B S T R A C T

While the eddy covariance (EC) technique is a well-established method for measuring water fluxes (i.e., evaporation or 'evapotranspiration', ET), the measurement is susceptible to many uncertainties. One such issue is the potential underestimation of ET when relative humidity (RH) is high (>70%), due to low-pass filtering with some EC systems. Yet, this underestimation for different types of EC systems (e.g. open-path or closed-path sensors) has not been characterized for synthesis datasets such as the widely used FLUXNET2015 dataset. Here, we assess the RH-associated underestimation of latent heat fluxes (LE, or ET) from different EC systems for 163 sites in the FLUXNET2015 dataset. We found that the LE underestimation is most apparent during hours when RH is higher than 70%, predominantly observed at sites using closed-path EC systems, but the extent of the LE underestimation is highly site-specific. We then propose a machine learning based method to correct for this underestimation, and compare it to two energy balance closure based LE correction approaches (Bowen ratio correction, BRC, and attributing all errors to LE). Our correction increases LE by 189% for closed-path sites at high RH (>90%), while BRC increases LE by around 30% for all RH conditions. Additionally, we assess the influence of these corrections on ET-based transpiration (T) estimates using two different ET partitioning methods. Results show opposite responses (increasing vs. slightly decreasing T-to-ET ratios, T/ET) between the two methods when comparing T based on corrected and uncorrected LE. Overall, our results demonstrate the existence of a high RH bias in water fluxes in the FLUXNET2015 dataset and suggest that this bias is a pronounced source of uncertainty in ET measurements to be considered when estimating ecosystem T/ET and WUE.

1. Introduction

Terrestrial evaporation or 'evapotranspiration' (ET) estimates (referring to the sum of all evaporation sources such as plant transpiration, T, as well as soil and surface evaporations, E) are important for understanding terrestrial ecosystems, and evaluating ecosystem and Earth system models (Fisher et al., 2017), as ET integrates many terrestrial biosphere processes, including the water cycle (E, T), carbon cycle (T and photosynthesis trade-off), and energy cycle (latent heat flux, hereafter, LE) (Monteith, 1965). Global and regional ET is often estimated from remote sensing process-based models (e.g., Miralles et al., 2011; Mu et al., 2007, Mu, 2011) and land surface models (e.g., Lawrence et al., 2007; Wartenburger et al., 2018), but these estimates are inconsistent and show high uncertainty (Miralles et al., 2016; Pan et al., 2020; Zhang et al., 2016).

One of the most common methods to measure ET at ecosystem scales is the eddy covariance (EC) technique, which can provide long-term, near-continuous, and high temporal resolution observations. However, water fluxes measured with EC systems suffer from potential errors related to low- and high-pass filtering (Foken, 2008; Franssen et al., 2010; Leuning et al., 2012; Mauder et al., 2020). Low-pass filtering errors are caused by, for instance, averaging over finite paths or volumes, the finite time response of instruments, sensor separation, and tube attenuation, which results in high-frequency signal loss (Fratini et al., 2012; Haslwanter et al., 2009; Ibrom et al., 2007; Mammarella et al., 2009; Massman and Ibrom, 2008). High-pass filtering errors result from a part of the flux being missed during the typical 30-min averaging period due to longer time-scale eddies, especially in tall canopies (Leuning et al., 2012; Mauder et al., 2020). The low-pass filtering may result in a flux loss that varies both by the type of the gas analyzer used: open-path and closed-path or enclosed-path infrared gas analyzers, as well as by the set-up of the sensors: inline/inlet filters (Nordbo et al., 2014), tube length for the closed-path and enclosed-path analyzers and tube heating, etc. For instance, closed-path analyzers in general work in almost all weather conditions and record data over a long time span. In contrast, open-path analyzers are more affected by adverse weather conditions (Haslwanter et al., 2009; Heusinkveld et al., 2008; Mauder et al., 2008) and for this reason, are more prone to missing data. However, open-path analyzers have the advantage of very low energy consumption, minimal maintenance requirements, and superior spectral response characteristics (Burba et al., 2008). Closed-path analyzers with long tubes suffer from additional low-pass filtering effects as relative humidity (RH) increases the need for corrections to avoid biases in measured LE (Foken, 2008; Franssen et al., 2010; Leuning et al., 2012; Mauder et al., 2020). Some studies simply removed the periods when RH exceeds 95% (Hu and Lei, 2021; Knauer et al., 2018; Li et al., 2019), however, although RH is usually elevated during and after rain events, it can also be high early in the morning, before rain events or independent of local rain. Therefore, RH-dependent corrections need to be applied to minimize the potential underestimation of LE. Ibrom et al. (2007) were the first to systematically describe the RH-dependent low-pass filtering effect and proposed an empirical approach to fit the spectral transfer function in RH bins. Then, a physical model was suggested to address this issue by Massman and Ibrom (2008) and became part of the community eddy covariance post-processing software EddyPro, but it is not clear whether, or, to what extent, this RH dependent low-pass filter correction has been routinely applied in the post-processing of the ET flux data. Therefore, within the FLUXNET2015 dataset, it remains unknown to which extent LE is underestimated at high levels of RH for each site.

EC measured ET is also often used as a reference to understand the physiological basis of water–carbon–energy coupling (Stoy et al., 2019; Xu et al., 2018; Zhang et al., 2019). As such, ET (or LE, in energy flux units, $W \cdot m^{-2}$) is an indispensable variable to derive key physiological parameters, such as surface or canopy conductance and the relationship between gross CO_2 assimilation and canopy conductance (inversely related to the marginal carbon cost of water to the plant) (Bonan et al., 2014; Groenendijk et al., 2011; Medlyn et al., 2017; Medlyn, 2011). However, this often requires the separation of the biological signal (T) from the total ET. Ecosystem T can be estimated by many observational techniques such as sap-flow measurements (hereafter T_{SAP}, Cammalleri et al., 2013; Poyatos et al., 2021, 2016), carbonyl sulfide uptake (Wehr et al., 2017), isotopes (Ma and Song, 2019; Xiao et al., 2018), or, by deploying above and below canopy EC systems (Paul-Limoges et al., 2020). These techniques tend to be limited by either monetary or labor expenses and have their own uncertainties as well as challenges when scaling plant level measurements to the ecosystem scale (Kool et al., 2014; Sun et al., 2019; Xiao et al., 2018). The relatively sparse availability of independent T measurements compared to the amount of EC data, such as in the widely used FLUXNET2015 dataset (Pastorello et al., 2017), has pushed the community to explore and develop approaches to separate T and E from EC measurements (Nelson et al., 2020; Scott et al., 2021; Stoy et al., 2019). For example, Zhou et al. (2016) and Nelson et al. (2018) proposed data-driven ET partitioning methods (Z16, *N18*), specifically designed to take advantage of the existing large amounts of EC data. Both *N18* and *Z16* estimate T based on estimating water use

efficiency (WUE) empirically. While these two approaches are rather simple to implement, they are sensitive to the uncertainties in input data (Nelson et al., 2020). Therefore, it is necessary to explore to which extent T/ET and WUE are affected by the uncertainties in the forcing ET.

In this study, we quantity (1) the extent to which hourly LE is underestimated from intermediate to high RH conditions (> 50% RH) for different types of EC systems in the FLUXNET2015 dataset. (2) We then propose a machine learning based empirical approach to correct LE underestimation under high RH conditions (the High Relative Humidity Correction, HRHC). (3) We also compare the HRHC approach with the most commonly used LE correction approaches, such as the Bowen ratio energy balance closure based LE correction (hereafter, BRC; Foken, 2008; Pastorello et al., 2020) and the approach of ascribing the residual errors of the energy balance closure entirely into LE (hereafter, AEIL; Amiro, 2009; Wohlfahrt and Widmoser, 2013). Next, (4) we apply two ET partitioning methods, *N18* and *Z16*, to estimate ecosystem T based on the uncorrected and corrected ET (in total three versions per partitioning method). Finally, (5) we compare the different versions of EC-based T estimates with independent sap flow based T estimates at the daily scale.

2. Data and method

2.1. EC data

EC measurements from 163 FLUXNET2015 sites (Pastorello et al., 2020) datasets were employed in this study (description of sites in supplementary Table S1), consisting of 54 sites with closed-path gas analyzers (hereafter, closed-path sites), 102 sites with open-path gas analyzers (hereafter, open-path sites), as well as 7 sites with enclosed-path gas analyzers (hereafter, enclosed-path sites). For the FLUXNET2015 sites which had updated data (after 2014) in the ICOS-2018 (Drought 2018 Team and ICOS Ecosystem Thematic Centre, 2020) data product, the data from ICOS-2018 was used to have a longer timeseries. Where possible, the sensor type was confirmed by the site principal investigator 'PI'. Since the number of enclosed-path EC sites was limited to only seven sites, the following sections focus primarily on open-path and closed-path EC sites when referring to the analysis among sites in the FLUXNET2015 dataset. At sites which changed sensors, the time periods with the longest continuous use with one sensor was used in the analysis.
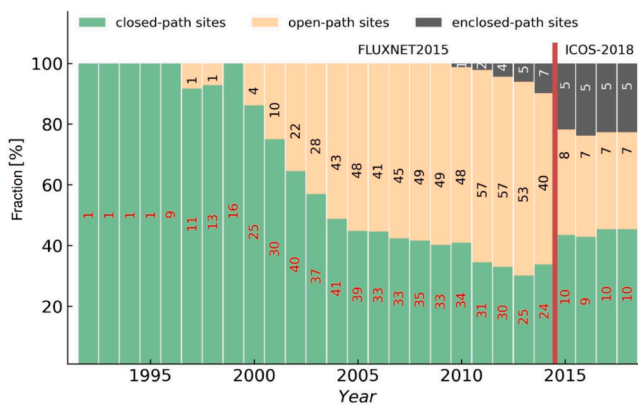

Fig. 1. Counts of open-, closed-, and enclosed-path sites from 1992 to 2014 in the FLUXNET2015 and 2015–2018 from ICOS-2018 datasets (if FLUXNET2015 sites are also in ICOS-2018 datasets). The number in each bar is the number of sites in that year. The y-axis is in percentage to highlight the ratio of sensors used in each year. The overall dataset is composed of two parts: FLUXNET2015 and ICOS-2018 starting from 2014. The bold red line represents the year 2014; Data from the ICOS-2018 dataset is retained for those sites that are represented in both datasets. (For interpretation of the references to color in this figure legend, the reader is referred to the web version of this article.)

Fig. 1 shows the number of sites for each year. Besides, we introduced two sites which have paired open-path and enclosed-path gas systems (due to the lack of the availability of paired open-path and closed-path systems), ES-LMa (Savannas) and IT-Trf (Deciduous Needleaf Forests), to better compare the RH-dependent effect for different sensors. Flux measurements and meteorological data, including net radiation (Rn, W·m^{-2}), sensible heat flux (H, W·m^{-2}), LE (W·m^{-2}), ground heat flux (G, W·m^{-2}), air temperature (TA, °C), and their related quality control flags, were used to perform the analysis. ET (mm·hour^{-1}) was derived from LE using the latent heat of vaporization as a function of TA ($ET = \frac{LE}{(2.501 - 0.00237 * TA) * 10^6}$, Stull, 1988). Estimates of GPP (μmol CO$_2$ m^{-2}·s^{-1}) were derived from partitioning algorithms based on nighttime net ecosystem exchange data (Reichstein et al., 2005). A more comprehensive list of variables (including variable descriptions) can be found in supplementary Table S2.

Since flux measurements are not available at the half-hourly scale for all participating sites, data were aggregated to hourly resolution for greater consistency. Periods with negative LE and low residual LE (Rn-H-G < 10 W·m^{-2}) were removed in the whole analysis. The friction velocity filter used for carbon flux was also applied to remove periods with 'low turbulence'. Moreover, periods with reported negative RH were excluded to reduce noise in the analysis. G was set to 0 to execute the HRHC for sites without G measurements (31 sites), because the effect of omitting G is very small compared to the overall variability and uncertainty (Figure S1).

2.2. Latent energy ratio and LE corrections

Based on the energy balance equation, the LE ratio (LER) is defined here as:

$$LER = \frac{LE}{Rn - H - G}. \tag{1}$$

where LER = 1 indicates a full energy balance closure. The storage term (energy in the air profile between ground surface and hygrometer, e.g., energy storage in the canopy) was not included in LER as it is challenging to measure and is not provided as a standard variable in the FLUXNET2015 and ICOS-2018 datasets. Even so, we explored the relevance of the storage terms in three selected sites (LE storage at two savanna sites with enclosed-path systems, ES-LM1 and ES-LM2, and both H storage and LE storage at one deciduous needle-leaf forest (IT-Trf), see Section 4.1 and Figure S7).

In this work, the proposed high relative humidity correction approach (HRHC) was compared to two other energy balance closure approaches (BRC and AEIL). The conceptual difference between the strategies of BRC and HRHC, as well as the flowchart of HRHC are shown in Fig. 2, with a detailed explanation of all approaches in the subsequent subsections.

2.2.1. High relative humidity correction (HRHC)

The HRHC (Zhang, 2022), based on a machine learning algorithm (eXtreme Gradient Boosting, Chen and Guestrin, 2016), was adopted to model the non-linear trend of LER along with RH. In this work, the algorithm was further set a negatively monotonical constrained by RH to enforce the decreasing response of LER to RH, due to the fact that the extent of LE underestimate increases with RH (Massman and Ibrom, 2008), meaning that only decreases in LER relative to RH were modeled. The correction is based on the predicted LER (LER_{pred}), which was modeled using only RH as a predictor, where LER_{pred} describes the general trend of decreasing LER with RH for the site (one model per site). Due to the skewed distribution of LER, which may bias the model performance, we trained and predicted logarithmically converted LER ($ln(LER)$):
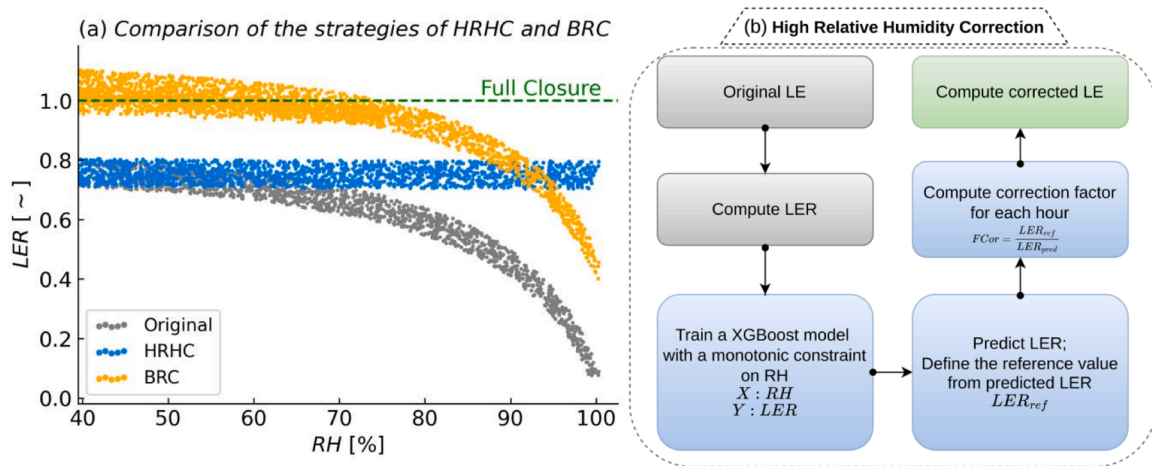
$$ln(LER) = f(RH). \tag{2}$$

Fig. 2. Conceptual strategies of HRHC and BRC at hourly scales (a) and the flowchart of HRHC (b). The dashed green line indicates the full energy balance closure at hourly scales. The gray points represent the original LE, the blue points represent LE after applying HRHC, and the orange points represent LE after applying BRC. Gray rectangles indicate the preparation for the original data, blue rectangles indicate the estimation of Fcor, and the green rectangle indicates the corrected LE. One schematic diagram is shown in Figure S2 to explain how to compute FCor. (For interpretation of the references to color in this figure legend, the reader is referred to the web version of this article.)

Based on the LER_{pred}, a reference value (LER_{ref}) for each site was determined as the LER_{pred} at (or closest to) 50% RH ($LER_{ref} = LER_{pred[RH\simeq50\%]}$),

$$LER_{ref} = LER_{pred[RH\simeq50\%]}. \tag{3}$$

Then, a correction factor (FCor) for each hourly measurement was calculated as the ratio of LER_{ref} to the corresponding LER_{pred} (based on RH for that hour).

$$FCor = \frac{LER_{ref}}{LER_{pred}}. \tag{4}$$

Finally, the corrected LE (LE_{cor}) was then calculated as the original (measured) LE multiplied by FCor, which is always greater than one. To prevent unexpected and extremely high levels of corrections, the maximum LE_{cor} was constrained to be below LE_{resid}, where LE_{resid} refers to residual LE from the energy balance closure equation ($Rn - H - G$),

$$LE_{cor} = min\big(LE_{original} * FCor, max\big(LE_{original}, LE_{resid}\big)\big). \tag{5}$$

2.2.2. Bowen ratio energy balance closure correction (BRC)

The BRC is widely used to achieve energy balance closure at daily scales, with the correction factors equally distributed to H and LE at sub-daily scales (Pastorello et al., 2020). Two key distinguishing differences between the BRC and HRHC are that 1) HRHC corrects only LE and only at high relative humidity compared to BRC that corrects LE and H independent of RH. This implies that the decreasing trend of LE with increasing RH remains after BRC (Fig. 2). 2) The HRHC does not enforce full energy balance closure like BRC but corrects LE at high RH to achieve an energy balance closure value typically observed at intermediate humidity at that site.

2.2.3. All errors in energy imbalance into LE correction (AEIL)

The LE estimate by AEIL was proposed based on the assumption that the other terms in the energy balance (i.e., Rn, H, and G) can be measured with sufficient accuracy and confidence, or assumed negligible, so that the lack of closure in the energy balance can be attributed to measurement deficiencies in LE (Amiro et al., 2006; Loescher et al., 2005), and this LE estimate was shown to be less accurate at the sub-daily scale than at the daily, weekly, and seasonal scales as there is more scatter among the daily data (Amiro, 2009). In this work, we aggregate the hourly data to daily data to diagnose if the LE estimate with this method is broadly applicable to FLUXNET2015 sites.

2.3. Methods for estimating transpiration (T)

2.3.1. Estimation of transpiration via Nelson et al. (2018, T_{N18})

The *N18* (Nelson et al., 2018) algorithm predicts plant WUE (WUE_{pred}, μmol CO_2 $mmol^{-1}$ H_2O) by training a model on the ecosystem WUE (GPP/ET) at the sub-daily scale using a quantile random forest model (Breiman, 2001; Meinshausen, 2006) during the periods when the surfaces are dry (i.e. surface evaporation is low) and plants are photosynthetically active. The estimated T (hereafter, T_{N18}) is then calculated using the WUE_{pred} from the model and the GPP ($T_{N18} = GPP/WUE_{pred}$). For more details see Nelson et al. (2018).

2.3.2. Estimation of transpiration via Zhou et al. (2016, T_{Z16})

The *Z16* (Zhou et al., 2016) algorithm was proposed based on the concept of uWUE (μmol CO_2 $hPa^{0.5}$ $mmol^{-1}$ H_2O) with consideration of the VPD effect at the ecosystem scale, which is defined as:

$$uWUE = \frac{GPP * \sqrt{VPD}}{ET}. \tag{6}$$

Two versions of uWUE are then estimated based on this concept: the potential uWUE (uWUEp) and the apparent uWUE (uWUEa), which are slopes from a quantile regression (at the 95th percentile) and linear regression, between $GPP \cdot \sqrt{VPD}$ and ET for a single year and each day in the year, respectively, so that ecosystem T (hereafter T_{Z16}) can be approximated by:

$$T_{Z16} = ET \cdot \frac{uWUEa}{uWUEp}. \tag{7}$$

2.3.3. Estimation of transpiration via sap flow

Sap flow data was collected from 10 sites in the SAPFLUXNET database (Poyatos et al., 2021) which are co-located with corresponding EC towers (four at open-path sites and six at closed-path sites, see Table S3). Plant T estimates were then upscaled to ecosystem-scale T following the description in Nelson et al. (2020), where the average normalized sap flow per unit basal area per species was multiplied by the basal area of each species in the stand and summed to total stand-level T. One key difference between Nelson et al. (2020) and the data here is that the upscaling was performed at hourly scales and then aggregated to daily T values rather than upscaling directly to daily values. To allow comparisons between the EC and sap flow based T estimates, the Pearson correlation was calculated in a bi-weekly step window between T_{SAP} and EC-based T (T_{N18} and T_{Z16}) to account for any temporal changes in

the sap flow measurement systems such as changes in the number of sensors or wounding effects.

3. Results

3.1. Original LER and corrected LER

3.1.1. Original LER

To assess the extent to which LE is affected by RH for open-path, closed-path and enclosed-path EC sites, we analyzed the trend of LER against binned RH (bins correspond to the central value, $\pm5\%$ RH, hereafter referenced only by the central value e.g. $RH_{55\%}$). As LER for different sites is not at the same amplitude, all LER data are reported as relative LER (RLER, relative to the median value at $RH_{55\%}$) for better comparability across sites.

Fig. 3 shows how the original (i.e. LE data directly reported from FLUXNET with no correction) RLER varies with RH across sites. The trend of original RLER shows a clear RH effect for all three EC system types at low and high RH conditions, while the magnitude is weaker for open-path sites at high RH compared to closed and enclosed-path sites, with RLER dropping to around 0.88 at $RH_{95\%}$ for the open-path sites. For closed-path sites, RLER decreased more markedly, reaching around 0.33 at $RH_{95\%}$. For enclosed-path sites, LE loss at high RH is even stronger than for closed-path sites, with a RLER of 0.27 at $RH_{95\%}$.

3.1.2. HRHC-based LER

Fig. 4 shows the FCor and HRHC-based RLER changes along RH bins. For all sites, FCor starts to exceed 1 around $RH_{65\%}$. For the closed-path and enclosed-path sites, the median values of FCor are higher than three at $RH_{95\%}$, while for open-path sites FCor is around 1.1. The RLER after applying HRHC for all sites is at, or slightly higher than, one for all bins above $RH_{35\%}$. The slightly higher median values result from the fact that the correction only increases LE thus leaving any errors where the measured LER was higher than would be expected, resulting in a slight positive correction bias (see Eq. (5)). However, the effect is small with a flat response of RLER to increasing RH. We also presented the distribution of FCor for 6 selected sites in Figure S3.

The absolute and relative changes in LE after applying HRHC are also presented in order to quantitatively examine the correction (Fig. 5). Correspondingly to Fig. 4a, the absolute and relative changes in LE also start to be positive from around $RH_{65\%}$. Meanwhile, the increase in LE fluxes for closed-path and enclosed-path sites are higher than for the open-path sites. For instance, at $RH_{95\%}$, the median values of absolute
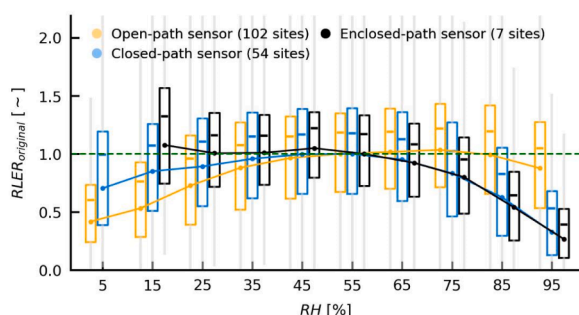

Fig. 3. The original relative LER (RLER) from all sites across RH bins at the hourly scale. RLER is LER relative to the median value at $RH_{55\%}$. The dots are the median value and the short horizontal lines are the mean value of the boxed data. The solid lines connect the median value to show that the overall pattern of RLER varies for open-, closed-, and enclosed-path sites. Boxes indicate interquartile ranges and gray vertical lines indicate the range of the data in each box. Data outside the interquartile range are not shown here to simplify the figure and clearly show the patterns. Bins with less than 500 h of data are not plotted. (For interpretation of the references to colour in this figure legend, the reader is referred to the web version of this article.)

changes in LE are 12 W·m^{-2} and 15 W·m^{-2} for closed-path and enclosed-path sites, respectively, while it is 3 W·m^{-2} for open-path sites. However, even though the absolute changes are not so dramatic, the relative changes for all types are pronounced, especially for the closed-path and enclosed-path sites (189% and 264%, respectively). The distribution of absolute changes in LE for six sites (Figure S4), and a comparison of original and corrected LE values for the same six sites (Figure S5) are also provided.

3.1.3. BRC-based LER

The BRC correction was already implemented in the FLUXNET2015 dataset according to the ONEFLUX pipeline. Here, we show the RLER using the provided data (Figure S6), and the changes in LE with BRC corrected data (Fig. 6). The RH-dependent errors still persist, and the most absolute changes in LE occur at moderate RH conditions for all sites. The relative changes in LE are almost constant across RH bins, consistent with the design of the method.

3.2. Influence of LE correction on EC-based T estimates

Fig. 7 shows the effect of the HRHC and BRC on T estimates from different partitioning methods (T_{N18}, T_{Z16}) in terms of the relative changes of T/ET and WUE (WUE = GPP/T) for both open-path (Fig. 7b, 7d) and closed-path sites (Fig. 7a, 7c). Overall, the *N18* method was more affected by the HRHC corrected LE than Z16, with the T_{N18}-based WUE being reduced by almost 18% at high RH conditions for closed-path sites and by 5% for open-path sites. Correspondingly, the T_{N18}-based T/ET was increased by 4% for closed-path sites. In contrast, the T_{Z16}-based WUE were only slightly affected and T/ET were reduced by 5% for closed-path sites after applying the HRHC. The main difference between the HRHC and BRC corrections was that, for the latter, WUE consistently decreased by 20–25% for both T partitioning methods across all RH conditions. Overall, the BRC correction had minimal influence on T/ET.

In order to evaluate the performance of the three correction methods, we compared EC-based T estimates to an independent T estimate, T_{SAP}. Fig. 8 shows correlation coefficients between T_{SAP} and EC-based T estimates (using both original ET, as well as HRHC, BRC, and AEIL corrected ET) by T_{N18} and T_{Z16} partitioning methods for both open-path and closed-path EC sites. Overall, there were no pronounced changes in the correlation with T_{SAP} between the HRHC and BRC compared to the uncorrected (original) T_{Z16} and T_{N18} for both open-path and closed-path sites. However, the relationship between T_{SAP} and EC-based T after AEIL correction was strongly compromised, indicating that simply attributing all residual energy to LE is inappropriate across all RH conditions, with the effect stronger for the *Z16* than the *N18* method.

4. Discussion

4.1. RH effect on LE measurements

The LER variations with RH in the FLUXNET2015 dataset show a systematic increase from low to intermediate RH conditions independent of sensor type. LER then decreases from intermediate to high RH, where this decline is substantially larger for closed-path and enclosed-path sensors compared to open-path sensors. In the following paragraphs, we discuss potential mechanisms for this pattern and their implications for systematic biases in eddy covariance based LE measurements.

LER measures the relative energy balance closure gap and reflects all potential errors in the accounting of the energy balance. Measurements of net radiation are typically much more accurate compared to the turbulent fluxes (LE and H) measured by eddy covariance and are thus unlikely to be a major source of a systematic bias (Foken, 2008; Mauder et al., 2020; Wilson et al., 2002). Mismatches of the radiometric and eddy covariance footprint can be contributing to the energy balance
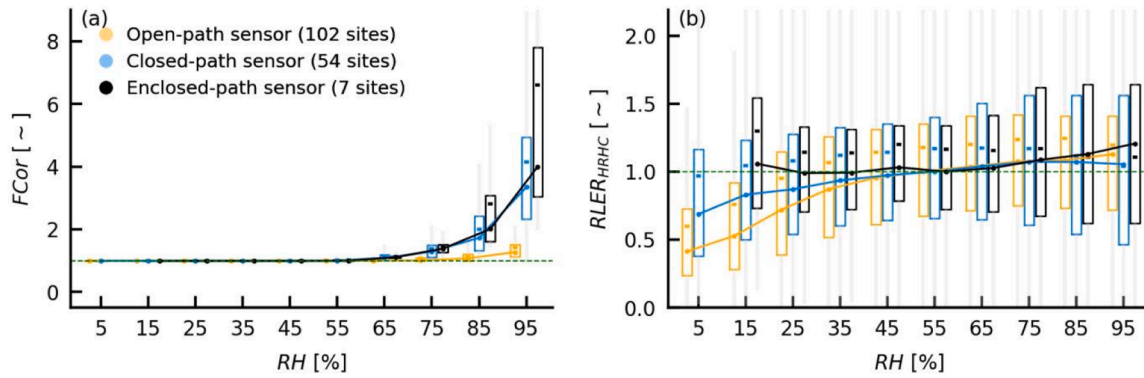
Fig. 4. (a) FCor and (b) HRHC-based relative LER (RLER) from all sites across RH bins at the hourly scale. The dots are the median value and the short horizontal lines are the mean value of the boxed data. The solid lines connect the median value to show the overall pattern. Boxes indicate interquartile ranges and gray vertical lines indicate the data ranges in each box. Data outside the interquartile range are not shown here to simplify the figure and clearly show the patterns. Bins with less than 500 h of data are not plotted. (For interpretation of the references to colour in this figure legend, the reader is referred to the web version of this article.)
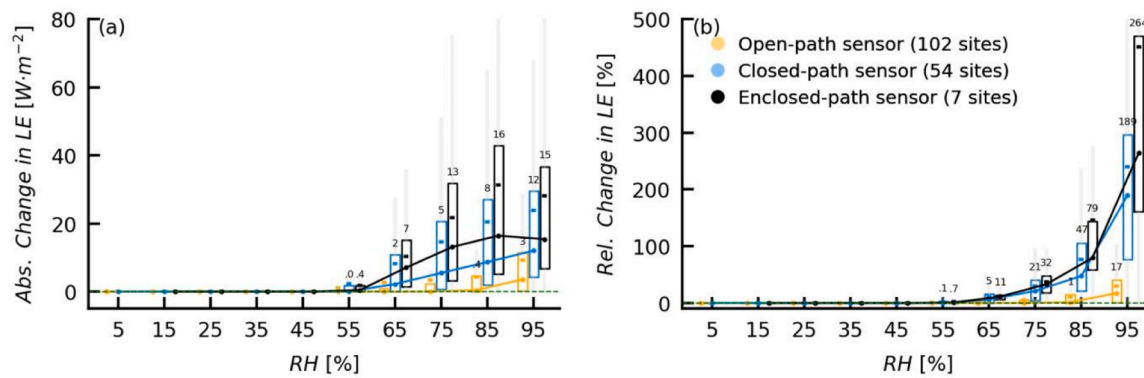

Fig. 5. (a) Absolute and (b) relative changes in LE after applying HRHC for all sites across RH bins at the hourly scale. The dots are the median value and the short horizontal lines are the mean value of the boxed data. The solid lines connect the median value. The numbers above boxes represent median values. Boxes indicate interquartile ranges and gray vertical lines indicate the ranges of the data in each box. Data outside the interquartile range are not shown here to simplify the figure and clearly show the patterns. Bins with less than 500 h of data are not plotted. (For interpretation of the references to colour in this figure legend, the reader is referred to the web version of this article.)
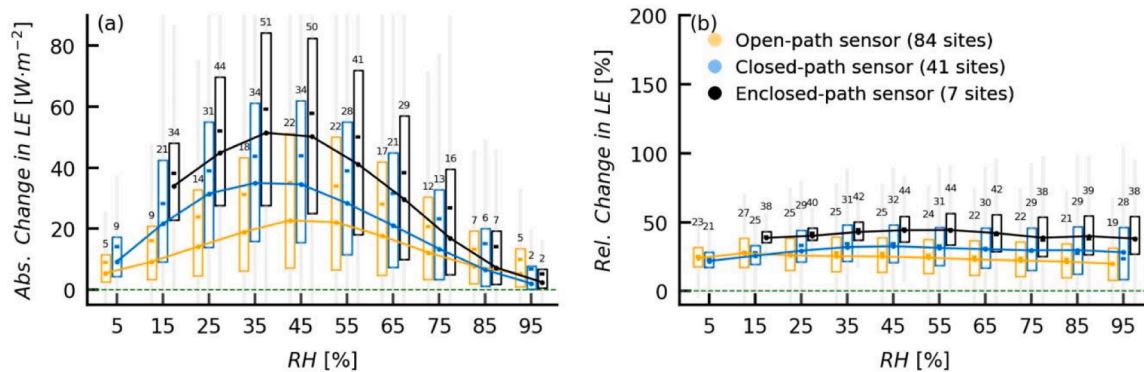

Fig. 6. (a) Absolute and (b) relative changes in LE from BRC corrected data for all sites across RH bins at the hourly scale. The numbers of close- and open-path sites are less than the numbers in previous figures as the BRC was not executed at several sites. The dots are the median value and the short horizontal lines are the mean value of the boxed data. The solid lines connect the median value. The numbers above boxes represent median values. Boxes indicate interquartile ranges and gray vertical lines indicate the ranges of the data in each box. Data outside the interquartile range are not shown here to simplify the figure and clearly show the patterns. Bins with less than 500 h of data are not plotted. (For interpretation of the references to colour in this figure legend, the reader is referred to the web version of this article.)

closure gap, in particular at individual times and for heterogeneous sites (Leuning et al., 2012; Mauder et al., 2020; Stoy et al., 2013), while it seems implausible that this could explain the large systematic energy balance closure gap observed across the entire network and the systematic pattern varying with RH. Likewise, uncertainties in the ground heat flux and the omission of other energy storage terms are also unlikely to play an important role in the overall systematic patterns of the energy balance closure gap across FLUXNET because they are
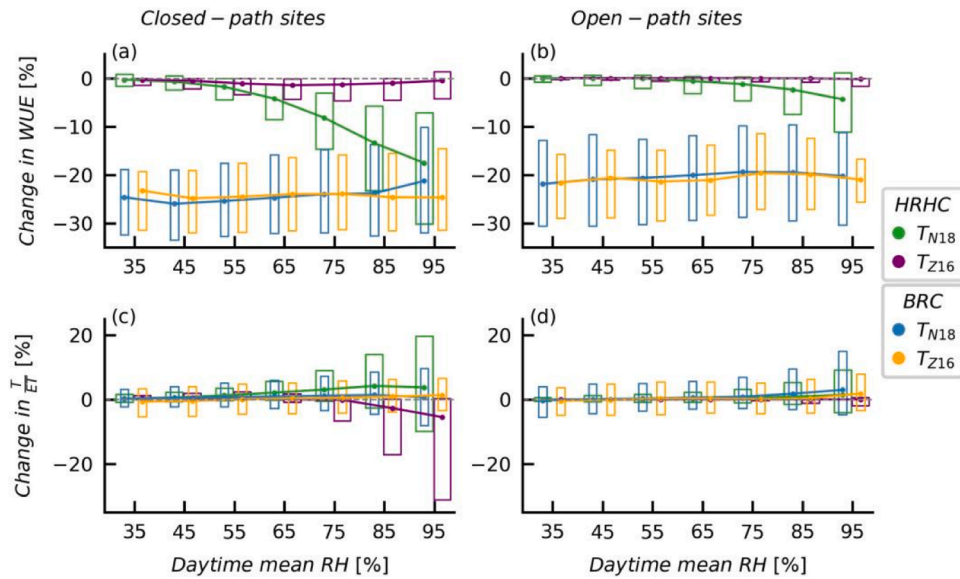
Fig. 7. Relative change of WUE (top row) and T/ET (bottom row) to daytime mean RH at daily scale for closed-path and open-path sites after the correction applied (HRHC, BRC). The dots are the median values which are connected by the solid lines. Only days with a mean temperature above 5 °C, at least 1 mm/day of ET, and where both partitioning methods could be applied, were included.
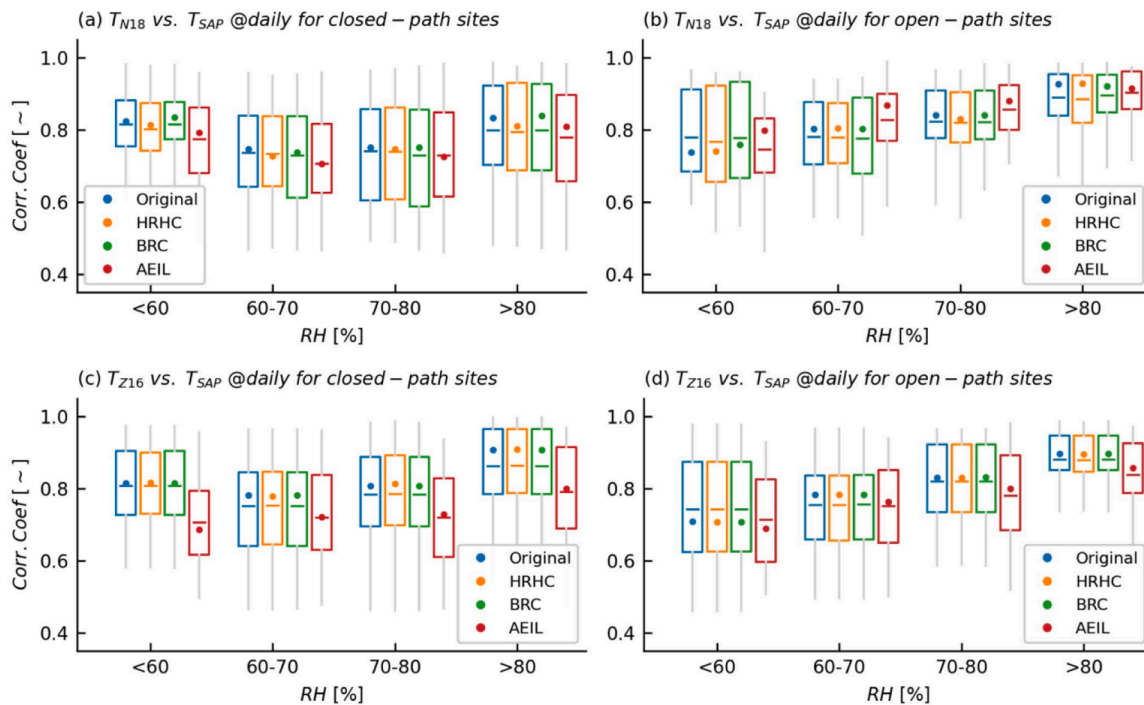

Fig. 8. Bi-weekly step window correlation analysis between TSAP and EC-based T against RH at the daily scale for closed-path (panels (a) and (c), 6 sites) and open-path (panels (b) and (d), 4 sites) sites. Note that for each box, data were filtered from all significant ($p < 0.1$) coefficients. The different color of the box indicates the correlation coefficients for EC-based T, which were estimated based on different versions of ET over all referred sites.

quantitatively too small (Wilson et al., 2002; Figure S1, S7).

Errors in measuring the vertical wind speed by the sonic anemometer under certain wind directions ("angle of attack") can cause systematic underestimation, in particular of H (Nakai et al., 2006; Nakai and Shimoyama, 2012). However, this cannot explain the observed pattern of LER with RH. Our finding of increasing LER from low to intermediate RH independent of sensor type is consistent with the mesoscale circulation hypothesis (Brötz et al., 2014; Mauder et al., 2007, 2008, 2021; Roo et al., 2018; Zhou et al., 2018) because the differential heating of the landscape triggering large-scale eddies becomes more important with

increasing dryness, reflected here by decreasing RH. Accepting this hypothesis implies that the energy balance closure gap at low RH is more attributable to errors in H rather than LE and thus justifies why our LE correction method operates only at high RH. The decreasing trend of LER from intermediate to high RH, along with the pronounced difference in severity of the decline between open-path and closed-path sensors, cannot be explained by the mesoscale circulation hypothesis, but points to biases related to the measurement instruments and setup.

A systematic underestimation of LE at high RH in closed-path systems is a known problem in the community. To account for this problem,

spectral correction methods have been developed and time lag corrections take the effect of RH specifically into account for closed-path sensors (Ibrom et al., 2007; Massman and Ibrom, 2008). The fact that we are still observing a large and systematic decline of LER at high RH in FLUXNET2015 suggests that spectral correction methods were not, or not properly, systematically applied, or do not fully correct for the observational biases. The spectral corrections are done by the site PIs before the standardized ONEFLUX processing (Pastorello et al., 2020). Our findings highlight the importance of documenting the choice and details of the applied spectral corrections and call for revisiting the problem along with a reprocessing of the data for future data releases.

Since enclosed-path gas analyzers were designed to combine the advantages of closed-path and open-path systems and minimize high-frequency attenuation errors (Burba et al., 2012; Metzger et al., 2015; Novick et al., 2013), it was surprising to see that the LER decline at high RH for enclosed-path analyzers was comparable to closed-path sensors. However, the set-up correction proposed by Metzger et al. (2015) and later routinely implemented, concerning heated intake tube and rain cup shape were probably not implemented in the datasets belonging to the current analysis. Therefore, the behavior of enclosed path analyzers has to be further evaluated. Accounting for RH in the spectral correction or not for one site shows a large impact on the LER decline with RH, and further indicates that the correction accounting for RH is still not fully effective at high RH (Figure S8).

The weak but systematic decline of LER from intermediate to high RH observed for open-path systems was unexpected because there is no sampling tube and associated attenuations of high frequencies. It could arise from sensors getting wet and contaminating the optical window as open-path sensors are exposed to an outdoor environment (Burba et al., 2008; Haslwanter et al., 2009; Heusinkveld et al., 2008). However, such conditions should be flagged and discarded automatically by the device. We also see no systematic difference between an open-path and an enclosed-path system that ran in parallel at ES-LMa (Figure S9), suggesting that this seems unlikely to explain the observed pattern.

Another possible explanation for the decline of LER from intermediate to high RH seen in open-path systems is due to violations of the EC theory due to weak turbulence that are expected to be more frequent under high RH conditions. Indeed, we found that the RLER decline with RH for open-path sites gets stronger when we retain data with low turbulence (Figure S10), which implies that low turbulence errors are likely impacting H and LE measurements in all eddy covariance systems and that the u*-filtering for carbon exchange should also be applied to energy fluxes in the future. However, the HRHC correction also utilized the u*-filtering filter from the NEE quality flags to avoid including such errors in the correction. Ruling out rain or low turbulence errors, another plausible explanation is the separation of the water concentration measurements and the sonic anemometer, because particular atmospheric conditions like stable stratification paired with a weak flux and signal pose large challenges for spectral corrections that appear to be not fully effective (Heusinkveld et al., 2008). Given that the temperature measurements often come directly from the sonic anemometer while water concentration measurements come from the open-path gas analyzer, separation could also indicate that energy balance non-closure at high RH conditions are more related to LE for open-path systems, thus justifying the HRHC correction in all cases, though more detailed studies would be required to confirm this hypothesis.

The underestimation of LE at high RH implies also a likely systematic underestimation of interception evaporation, as rainfall coincides with high RH (van Dijk et al., 2015). We quantified the absolute and relative changes in corrected LE during rain events and during the following 3 h for the closed-path and enclosed path sites, showing that LE increased by 11 W·m^{-2} (0.38 mm/day in water flux units) and 16 W·m^{-2} (0.55 mm/day in water flux units) for the closed-path sites and enclosed-path sites, respectively (Figure S11).

In summary, the most plausible explanations for the observed systematic variations of LER with RH are: (1) the underrepresentation of large-scale eddies due to mesoscale circulations causing an underestimation of primarily H at the range of low to intermediate RH, and (2): remaining issues with spectral corrections causing underestimation of LE at the range of intermediate to high RH, which is much more severe for closed-path and enclosed-path compared to open-path systems. The proposed HRHC corrects the systematic LE underestimation at high RH to a typical energy balance closure level of the site, while it does not force full energy balance closure due to the expected biases in H, and to a lesser extent in LE, that are not accounted for (Fig. 4). The majority of the LE underestimation effect is expected to be dependent on the frequency of maintaining/replacing tubes and filters, thus the proposed HRHC could be done in corresponding temporal segments if these dates would be available as metadata. The BRC method forces full closure assuming an unbiased Bowen ratio, while the above considerations make clear that there are systematic biases in the measured Bowen ratio along the RH gradient. As a consequence, LE corrected by the Bowen ratio still shows systematic biases with RH. Likewise, there is no theoretical justification for the residual approach (AEIL), especially for low and intermediate RH conditions that are most frequent overall. Thus, correcting LE according to AEIL causes overestimation of LE that seems implausible (Fig. 4, Jung et al., 2019) and can also deteriorate the correspondence to sap flux measurements (Fig. 8).

4.2. Effect of LE correction on T estimation

The different influences of HRHC on T estimated by *N18* and *Z16* can be explained by the different mechanisms of the two algorithms (Fig. 7). While the *N18* method allows WUE dynamics to be flexible in time, the flexible nature also comes with the risk of the method becoming sensitive to errors in the training data (Nelson et al., 2018). For instance, *N18* trains a model on the WUEe (GPP/ET) during the growing seasons (GPP is greater than 0.05 μmol·C·m^{-2}·s^{-1} for each half hour and greater than 0.5 gC·m^{-2}·day^{-1} for each day, in addition to TA being higher than 5 °C for each half hour) with dry surfaces. The mask for filtering the periods is not directly related to RH, but estimated from surface wetness instead. Therefore, the LE values at high RH conditions are also selected to train the model in the algorithm. Any errors in the estimated LE would influence in the calculated WUEe the model is trained on and would be reflected in the predicted WUE used to calculate T. In the case of high RH errors, the underestimated original LE would result in an overestimated predicted WUE and thus lower T estimates, meaning the estimated WUE from *N18* is lower after applying HRHC at high RH (see Fig. 7). In contrast, for the *Z16* method, T estimates are based on WUE calculated via an estimated slope between the LE (ET) and GPP which is predominantly influenced by large fluxes, and thus the HRHC corrections which are mainly associated with small magnitudes have a minimal impact on the resulting T estimates. Therefore, the effects of the HRHC correction are primarily seen in the T/ET values, as the increases in ET from the correction are only seen in the denominator. In the case of the BRC correction, as all LE values are increased uniformly, both the *N18* and *Z16* methods attribute the increase to WUE and the T/ET ratios are relatively unchanged.

Though the influence of the HRHC correction on T estimates is different among the two ET partitioning methods, the overall changes in estimated patterns of T are relatively small compared to other potential sources of uncertainty. The analysis with sap flow (Fig. 8) also supports this interpretation, as the correlation coefficients remain unchanged for the original, HRHC, and BRC correction methods across all RH bins, with the exception of the AEIL correction. Thus, in the context of T estimations, the differences between most LE corrections are a small factor compared to the uncertainties in the scale differences when comparing sap flow and eddy covariance measurements. Likely a multifaceted approach, such as comparisons between LE and weighing lysimeters (Mauder et al., 2021; Paulus et al., 2021) and broader scale comparison between T estimates from EC and independent data sources, might have the potential to help understand the potential errors in EC-based T

estimates.

5. Conclusion

We analyzed the influence of gas analysis types for 163 sites in the FLUXNET2015 dataset on potential errors influencing the measured water vapor fluxes. Closed-path gas analyzers dominated the network until around the year 2000 when open-path gas analyzers became available and then widely used. We confirmed that the underestimation of hourly LE at high RH (RH > 70%) is observed in the FLUXNET2015, particularly with closed-path EC sites. We also reported that LE is underestimated, to a lesser extent, under high RH conditions at sites with open-path gas analyzers. While the systematic errors in closed-path systems found in the synthesis dataset are likely primarily attributed to tube effects, the underlying mechanisms for RH-related errors impacting all systems still need to be comprehensively investigated.

The proposed High Relative Humidity Correction provides a flexible machine-learning approach to consistently correct LE estimates from different EC systems for the existing error at high RH conditions. In contrast, current methods to correct energy balance closure in the existing dataset, such as the Bowen ratio based energy balance closure and energy balance residual methods, close the energy budget but are not justified by the state-of-the-art understanding of the energy balance closure gap. The T estimates from two ET partitioning methods showed contracting responses to the LE corrections, however the changes were relatively small overall in magnitude, particularly when compared to the uncertainties of comparing EC and sap flow based estimates of T.

In closing, the high RH errors in LE are present in the existing synthesis and broadly used data, like the FLUXNET2015 dataset (the focused dataset of the current study). These errors will remain in future datasets if not correctly addressed by the setup (heating) of sensors and processing (spectral corrections) of data. For this reason, future studies based on energy fluxes should take these effects into consideration. In addition, it is advisable, whenever possible, to re-process the EC raw data by applying one of the available spectral corrections that take into consideration the RH, and in general, it is crucial to save and share the metadata related to the set-up (type of IRGA) and processing applied.

Declaration of Competing Interest

The authors declare that they have no known competing financial interests or personal relationships that could have appeared to influence the work reported in this paper.

Data availability

Data can be downloaded from the FLUXNET2015 and ICOS-2018 websites. The code for applying High Relative Humidity Correction is in https://doi.org/10.5281/zenodo.7083230

Acknowledgments

Supplementary materials

Supplementary material associated with this article can be found, in the online version, at doi:10.1016/j.agrformet.2022.109305.

References

Amiro, B., 2009. Measuring boreal forest evapotranspiration using the energy balance residual. J. Hydrol. (Amst.) 366, 112–118. https://doi.org/10.1016/j.jhydrol.2008.12.021.

Amiro, B.D., Barr, A.G., Black, T.A., Iwashita, H., Kljun, N., McCaughey, J.H., Morgenstern, K., Murayama, S., Nesic, Z., Orchansky, A.L., Saigusa, N., 2006. Carbon, energy and water fluxes at mature and disturbed forest sites, Saskatchewan, Canada. Agric. For. Meteorol. 136, 237–251. https://doi.org/10.1016/j.agrformet.2004.11.012. Advances in Surface-Atmosphere Exchange - A Tribute to Marv Wesely.

Bonan, G.B., Williams, M., Fisher, R.A., Oleson, K.W., 2014. Modeling stomatal conductance in the earth system: linking leaf water-use efficiency and water transport along the soil–plant–atmosphere continuum. Geosci. Model Dev. 7, 2193–2222. https://doi.org/10.5194/gmd-7-2193-2014.

Breiman, L., 2001. Random Forests. Mach. Learn. 45, 5–32. https://doi.org/10.1023/A:1010933404324.

Brötz, B., Eigenmann, R., Dörnbrack, A., Foken, T., Wirth, V., 2014. Early-morning flow transition in a valley in low-mountain terrain under clear-sky conditions. Boundary-Layer Meteorol. 152, 45–63. https://doi.org/10.1007/s10546-014-9921-7.

Burba, G., Schmidt, A., Scott, R.L., Nakai, T., Kathilankal, J., Fratini, G., Hanson, C., Law, B., McDermitt, D.K., Eckles, R., Furtaw, M., Velgersdyk, M., 2012. Calculating CO2 and H2O eddy covariance fluxes from an enclosed gas analyzer using an instantaneous mixing ratio. Glob. Chang. Biol. 18, 385–399. https://doi.org/10.1111/j.1365-2486.2011.02536.x.

Burba, G.G., McDERMITT, D.K., Grelle, A., Anderson, D.J., Xu, L., 2008. Addressing the influence of instrument surface heat exchange on the measurements of CO2 flux from open-path gas analyzers. Glob. Chang. Biol. 14, 1854–1876. https://doi.org/10.1111/j.1365-2486.2008.01606.x.

Cammalleri, C., Rallo, G., Agnese, C., Ciraolo, G., Minacapilli, M., Provenzano, G., 2013. Combined use of eddy covariance and sap flow techniques for partition of ET fluxes and water stress assessment in an irrigated olive orchard. Agric. Water Manage., Soil Irrig. Sustain. Pract. 120, 89–97. https://doi.org/10.1016/j.agwat.2012.10.003.

Chen, T., Guestrin, C., 2016. XGBoost: a scalable tree boosting system. In: Proceedings of the 22nd ACM SIGKDD International Conference on Knowledge Discovery and Data Mining, KDD '16. Association for Computing Machinery, New York, NY, USA, pp. 785–794. https://doi.org/10.1145/2939672.2939785.

Drought 2018 Team and ICOS Ecosystem Thematic Centre, 2020. Drought-2018 Ecosystem Eddy Covariance Flux Product For 52 Stations in FLUXNET-Archive Format. https://doi.org/10.18160/YVR0-4898.

Fisher, J.B., Melton, F., Middleton, E., Hain, C., Anderson, M., Allen, R., McCabe, M.F., Hook, S., Baldocchi, D., Townsend, P.A., Kilic, A., Tu, K., Miralles, D.D., Perret, J., Lagouarde, J.-P., Waliser, D., Purdy, A.J., French, A., Schimel, D., Famiglietti, J.S., Stephens, G., Wood, E.F., 2017. The future of evapotranspiration: global requirements for ecosystem functioning, carbon and climate feedbacks, agricultural management, and water resources. Water Resour. Res. 53, 2618–2626. https://doi.org/10.1002/2016WR020175.

Foken, T., 2008. The energy balance closure problem: an overview. Ecol. Appl. 18, 1351–1367. https://doi.org/10.1890/06-0922.1.

Franssen, H.J.H., Stöckli, R., Lehner, I., Rotenberg, E., Seneviratne, S.I., 2010. Energy balance closure of eddy-covariance data: a multisite analysis for European FLUXNET stations. Agric. For. Meteorol. 150, 1553–1567. https://doi.org/10.1016/j.agrformet.2010.08.005.

Fratini, G., Ibrom, A., Arriga, N., Burba, G., Papale, D., 2012. Relative humidity effects on water vapour fluxes measured with closed-path eddy-covariance systems with short sampling lines. Agric. For. Meteorol. 165, 53–63. https://doi.org/10.1016/j.agrformet.2012.05.018.

Groenendijk, M., Dolman, A.J., van der Molen, M.K., Leuning, R., Arneth, A., Delpierre, N., Gash, J.H.C., Lindroth, A., Richardson, A.D., Verbeeck, H., Wohlfahrt, G., 2011. Assessing parameter variability in a photosynthesis model within and between plant functional types using global Fluxnet eddy covariance data. Agric. For. Meteorol. 151, 22–38. https://doi.org/10.1016/j.agrformet.2010.08.013.

Haslwanter, A., Hammerle, A., Wohlfahrt, G., 2009. Open-path vs. closed-path eddy covariance measurements of the net ecosystem carbon dioxide and water vapour exchange: a long-term perspective. Agric. For. Meteorol. 149, 291–302. https://doi.org/10.1016/j.agrformet.2008.08.011.

Heusinkveld, B.G., Jacobs, A.F.G., Holtslag, A.A.M., 2008. Effect of open-path gas analyzer wetness on eddy covariance flux measurements: a proposed solution. Agric. For. Meteorol. 148, 1563–1573. https://doi.org/10.1016/j.agrformet.2008.05.010.

Hu, X., Lei, H., 2021. Evapotranspiration partitioning and its interannual variability over a winter wheat-summer maize rotation system in the North China Plain. Agric. For. Meteorol. 310, 108635 https://doi.org/10.1016/j.agrformet.2021.108635.

Ibrom, A., Dellwik, E., Flyvbjerg, H., Jensen, N.O., Pilegaard, K., 2007. Strong low-pass filtering effects on water vapour flux measurements with closed-path eddy correlation systems. Agric. For. Meteorol. 17 https://doi.org/10.1016/j.agrformet.2007.07.007.

Jung, M., Koirala, S., Weber, U., Ichii, K., Gans, F., Camps-Valls, G., Papale, D., Schwalm, C., Tramontana, G., Reichstein, M., 2019. The FLUXCOM ensemble of global land-atmosphere energy fluxes. Sci. Data 6, 74. https://doi.org/10.1038/s41597-019-0076-8.

Knauer, J., Zaehle, S., Medlyn, B.E., Reichstein, M., Williams, C.A., Migliavacca, M., De Kauwe, M.G., Werner, C., Keitel, C., Kolari, P., Limousin, J.-.M., Linderson, M.-.L., 2018. Towards physiologically meaningful water-use efficiency estimates from eddy covariance data. Glob. Chang. Biol. 24, 694–710. https://doi.org/10.1111/gcb.13893.

Kool, D., Agam, N., Lazarovitch, N., Heitman, J.L., Sauer, T.J., Ben-Gal, A., 2014. A review of approaches for evapotranspiration partitioning. Agric. For. Meteorol. 184, 56–70. https://doi.org/10.1016/j.agrformet.2013.09.003.

Lawrence, D.M., Thornton, P.E., Oleson, K.W., Bonan, G.B., 2007. The Partitioning of Evapotranspiration into Transpiration, Soil Evaporation, and Canopy Evaporation in a GCM: impacts on Land–Atmosphere Interaction. J. Hydrometeorol. 8, 862–880. https://doi.org/10.1175/JHM596.1.

Leuning, R., van Gorsel, E., Massman, W.J., Isaac, P.R., 2012. Reflections on the surface energy imbalance problem. Agric. For. Meteorol. 156, 65–74. https://doi.org/10.1016/j.agrformet.2011.12.002.

Li, X., Gentine, P., Lin, C., Zhou, S., Sun, Z., Zheng, Y., Liu, J., Zheng, C., 2019. A simple and objective method to partition evapotranspiration into transpiration and evaporation at eddy-covariance sites. Agric. For. Meteorol. 265, 171–182. https://doi.org/10.1016/j.agrformet.2018.11.017.

Loescher, H.W., Gholz, H.L., Jacobs, J.M., Oberbauer, S.F., 2005. Energy dynamics and modeled evapotranspiration from a wet tropical forest in Costa Rica. J. Hydrol. (Amst.) 315, 274–294. https://doi.org/10.1016/j.jhydrol.2005.03.040.

Ma, Y., Song, X., 2019. Applying stable isotopes to determine seasonal variability in evapotranspiration partitioning of winter wheat for optimizing agricultural management practices. Sci.Total Environ. 654, 633–642. https://doi.org/10.1016/j.scitotenv.2018.11.176.

Mammarella, I., Launiainen, S., Gronholm, T., Keronen, P., Pumpanen, J., Rannik, U.L., Vesala, T., 2009. Relative humidity effect on the high-frequency attenuation of water vapor flux measured by a closed-path eddy covariance system. J. Atmos. Oceanic Technol. 26, 11. https://doi.org/10.1175/2009JTECHA1179.1.

Massman, W.J., Ibrom, A., 2008. Attenuation of concentration fluctuations of water vapor and other trace gases in turbulent tube flow. Atmos. Chem. Phys. 8, 6245–6259. https://doi.org/10.5194/acp-8-6245-2008.

Mauder, M., Desjardins, R.L., MacPherson, I., 2007. Scale analysis of airborne flux measurements over heterogeneous terrain in a boreal ecosystem. J. Geophys. Res. 112 https://doi.org/10.1029/2006JD008133.

Mauder, M., Desjardins, R.L., Pattey, E., Gao, Z., van Haarlem, R., 2008. Measurement of the sensible eddy heat flux based on spatial averaging of continuous ground-based observations. Bound.-Layer Meteorol. 128, 151–172. https://doi.org/10.1007/s10546-008-9279-9.

Mauder, M., Foken, T., Cuxart, J., 2020. Surface-energy-balance closure over land: a review. Bound.-Layer Meteorol. 177, 395–426. https://doi.org/10.1007/s10546-020-00529-6.

Mauder, M., Ibrom, A., Wanner, L., De Roo, F., Brugger, P., Kiese, R., Pilegaard, K., 2021. Options to correct local turbulent flux measurements for large-scale fluxes using an approach based on large-eddy simulation. Atmos. Meas. Tech. 14, 7835–7850. https://doi.org/10.5194/amt-14-7835-2021.

Medlyn, B.E., De Kauwe, M.G., Lin, Y.-.S., Knauer, J., Duursma, R.A., Williams, C.A., Arneth, A., Clement, R., Isaac, P., Limousin, J.-.M., Linderson, M.-.L., Meir, P., Martin-StPaul, N., Wingate, L., 2017. How do leaf and ecosystem measures of water-use efficiency compare? New Phytol. 216, 758–770. https://doi.org/10.1111/nph.14626.

Medlyn, B.E., Duursma, R.A., Eamus, D., Ellsworth, D.S., Prentice, I.C., Barton, C.V.M., Crous, K.Y., De Angelis, P., Freeman, M., Wingate, L., 2011. Reconciling the optimal and empirical approaches to modelling stomatal conductance. Glob. Chang. Biol. 17, 2134–2144. https://doi.org/10.1111/j.1365-2486.2010.02375.x.

Meinshausen, N., 2006. Quantile regression forests. J. Mach. Learn. Res. 7, 983–999.

Metzger, S., Burba, G., Burns, S., Blanken, P., Li, J., Luo, H., Zulueta, R., 2015. Optimization of a gas sampling system for measuring eddy-covariance fluxes of H2O and CO2. Atmos. Meas. Tech. 8, 10983–11028. https://doi.org/10.5194/amtd-8-10983-2015.

Miralles, D.G., Holmes, T.R.H., De Jeu, R.A.M., Gash, J.H., Meesters, A.G.C.A., Dolman, A.J., 2011. Global land-surface evaporation estimated from satellite-based observations. Hydrol. Earth Syst. Sci. 15, 453–469. https://doi.org/10.5194/hess-15-453-2011.

Miralles, D.G., Jiménez, C., Jung, M., Michel, D., Ershadi, A., McCabe, M.F., Hirschi, M., Martens, B., Dolman, A.J., Fisher, J.B., Mu, Q., Seneviratne, S.I., Wood, E.F., Fernández-Prieto, D., 2016. The WACMOS-ET project – Part 2: evaluation of global terrestrial evaporation data sets. Hydrol. Earth Syst. Sci. 20, 823–842. https://doi.org/10.5194/hess-20-823-2016.

Monteith, J.L., 1965. Evaporation and environment. Symp. Soc. Exp. Biol. 19, 205–234.

Mu, Q., Heinsch, F.A., Zhao, M., Running, S.W., 2007. Development of a global evapotranspiration algorithm based on MODIS and global meteorology data. Remote Sens. Environ. 111, 519–536. https://doi.org/10.1016/j.rse.2007.04.015.

Mu, Q., Zhao, M., Running, S.W., 2011. Improvements to a MODIS global terrestrial evapotranspiration algorithm. Remote Sens. Environ. 115, 1781–1800. https://doi.org/10.1016/j.rse.2011.02.019.

Nakai, T., Shimoyama, K., 2012. Ultrasonic anemometer angle of attack errors under turbulent conditions. Agric. For. Meteorol. 162–163, 14–26. https://doi.org/10.1016/j.agrformet.2012.04.004.

Nakai, T., van der Molen, M.K., Gash, J.H.C., Kodama, Y., 2006. Correction of sonic anemometer angle of attack errors. Agric. For. Meteorol. 136, 19–30. https://doi.org/10.1016/j.agrformet.2006.01.006.

Nelson, J.A., Carvalhais, N., Cuntz, M., Delpierre, N., Knauer, J., Ogée, J., Migliavacca, M., Reichstein, M., Jung, M., 2018. Coupling water and carbon fluxes to constrain estimates of transpiration: the TEA algorithm. J. Geophys. Res. 123, 3617–3632. https://doi.org/10.1029/2018JG004727.

Nelson, J.A., Pérez-Priego, O., Zhou, S., Poyatos, R., Zhang, Y., Blanken, P.D., Gimeno, T. E., Wohlfahrt, G., Desai, A.R., Gioli, B., Limousin, J., Bonal, D., Paul-Limoges, E., Scott, R.L., Varlagin, A., Fuchs, K., Montagnani, L., Wolf, S., Delpierre, N., Berveiller, D., Gharun, M., Belelli Marchesini, L., Gianelle, D., Šigut, L., Mammarella, I., Siebicke, L., Andrew Black, T., Knohl, A., Hörtnagl, L., Magliulo, V., Besnard, S., Weber, U., Carvalhais, N., Migliavacca, M., Reichstein, M., Jung, M., 2020. Ecosystem transpiration and evaporation: insights from three water flux partitioning methods across FLUXNET sites. Glob. Change Biol. 26, 6916–6930. https://doi.org/10.1111/gcb.15314.

Nordbo, A., Kekäläinen, P., Siivola, E., Mammarella, I., Timonen, J., Vesala, T., 2014. Sorption-caused attenuation and delay of water vapor signals in eddy-covariance sampling tubes and filters. J. Atmosph. Oceanic Technol. 31, 2629–2649. https://doi.org/10.1175/JTECH-D-14-00056.1.

Novick, K.A., Walker, J., Chan, W.S., Schmidt, A., Sobek, C., Vose, J.M., 2013. Eddy covariance measurements with a new fast-response, enclosed-path analyzer: spectral characteristics and cross-system comparisons. Agric. For. Meteorol. 181, 17–32. https://doi.org/10.1016/j.agrformet.2013.06.020.

Pan, S., Pan, N., Tian, H., Friedlingstein, P., Sitch, S., Shi, H., Arora, V.K., Haverd, V., Jain, A.K., Kato, E., Lienert, S., Lombardozzi, D., Ottlé, C., Poulter, B., Zaehle, S., Running, S.W., 2020. Evaluation of global terrestrial evapotranspiration using state-of-the-art approaches in remote sensing, machine learning and land surface modeling. Hydrol. Earth Syst. Sci. 25 https://doi.org/10.5194/hess-24-1485-2020.

Pastorello, G., Trotta, C., Canfora, E., Chu, H., Christianson, D., Cheah, Y.-.W., Poindexter, C., Chen, J., Elbashandy, A., Humphrey, M., Isaac, P., Polidori, D., Reichstein, M., Ribeca, A., van Ingen, C., Vuichard, N., Zhang, L., Amiro, B., Ammann, C., Arain, M.A., Ardö, J., Arkebauer, T., Arndt, S.K., Arriga, N., Aubinet, M., Aurela, M., Baldocchi, D., Barr, A., Beamesderfer, E., Marchesini, L.B., Bergeron, O., Beringer, J., Bernhofer, C., Berveiller, D., Billesbach, D., Black, T.A., Blanken, P.D., Bohrer, G., Boike, J., Bolstad, P.V., Bonal, D., Bonnefond, J.-.M., Bowling, D.R., Bracho, R., Brodeur, J., Brümmer, C., Buchmann, N., Burban, B., Burns, S.P., Buysse, P., Cale, P., Cavagna, M., Cellier, P., Chen, S., Chini, I., Christensen, T.R., Cleverly, J., Collalti, A., Consalvo, C., Cook, B.D., Cook, D., Coursolle, C., Cremonese, E., Curtis, P.S., D'Andrea, E., da Rocha, H., Dai, X., Davis, K.J., Cinti, B.D., Grandcourt, A., de, Ligne, A.D., De Oliveira, R.C., Delpierre, N., Desai, A.R., Di Bella, C.M., Tommasi, P, di, Dolman, H., Domingo, F., Dong, G., Dore, S., Duce, P., Dufrêne, E., Dunn, A., Dušek, J., Eamus, D., Eichelmann, U., ElKhidir, H.A.M., Eugster, W., Ewenz, C.M., Ewers, B., Famulari, D., Fares, S., Feigenwinter, I., Feitz, A., Fensholt, R., Filippa, G., Fischer, M., Frank, J., Galvagno, M., Gharun, M., Gianelle, D., Gielen, B., Gioli, B., Gitelson, A., Goded, I., Goeckede, M., Goldstein, A.H., Gough, C.M., Goulden, M.L., Graf, A., Griebel, A., Gruening, C., Grünwald, T., Hammerle, A., Han, S., Han, X., Hansen, B.U., Hanson, C., Hatakka, J., He, Y., Hehn, M., Heinesch, B., Hinko-Najera, N., Hörtnagl, L., Hutley, L., Ibrom, A., Ikawa, H., Jackowicz-Korczynski, M., Janouš, D., Jans, W., Jassal, R., Jiang, S., Kato, T., Khomik, M., Klatt, J., Knohl, A., Knox, S., Kobayashi, H., Koerber, G., Kolle, O., Kosugi, Y., Kotani, A., Kowalski, A., Kruijt, B., Kurbatova, J., Kutsch, W.L., Kwon, H., Launiainen, S., Laurila, T., Law, B., Leuning, R., Li, Yingnian, Liddell, M., Limousin, J.-.M., Lion, M., Liska, A.J., Lohila, A., López-Ballesteros, A., López-Blanco, E., Loubet, B., Loustau, D., Lucas-Moffat, A., Lüers, J., Ma, S., Macfarlane, C., Magliulo, V., Maier, R., Mammarella, I., Manca, G., Marcolla, B., Margolis, H.A., Marras, S., Massman, W., Mastepanov, M., Matamala, R., Matthes, J.H., Mazzenga, F., McCaughey, H., McHugh, I., McMillan, A.M.S., Merbold, L., Meyer, W., Meyers, T., Miller, S.D., Minerbi, S., Moderow, U., Monson, R.K., Montagnani, L., Moore, C.E., Moors, E., Moreaux, V., Moureaux, C., Munger, J.W., Nakai, T., Neirynck, J., Nesic, Z., Nicolini, G., Noormets, A., Northwood, M., Nosetto, M., Nouvellon, Y., Novick, K., Oechel, W., Olesen, J.E., Ourcival, J.-.M., Papuga, S.A., Parmentier, F.-.J., Paul-Limoges, E., Pavelka, M., Peichl, M., Pendall, E., Phillips, R.P., Pilegaard, K., Pirk, N., Posse, G., Powell, T., Prasse, H., Prober, S.M., Rambal, S., Rannik, Ü., Raz-Yaseef, N., Rebmann, C., Reed, D., Dios, V.R, de, Restrepo-Coupe, .N.., Reverter, B.R., Roland, M., Sabbatini, S., Sachs, T., Saleska, S.R., Sánchez-Cañete, E.P., Sanchez-Mejia, Z.M., Schmid, H.P., Schmidt, M., Schneider, K., Schrader, F., Schroder, I., Scott, R.L., Sedlák, P., Serrano-Ortíz, P., Shao, C., Shi, P., Shironya, I., Siebicke, L., Šigut, L., Silberstein, R., Sirca, C., Spano, D., Steinbrecher, R., Stevens, R.M., Sturtevant, C., Suyker, A., Tagesson, T., Takanashi, S., Tang, Y., Tapper, N., Thom, J., Tomassucci, M., Tuovinen, J.-.P., Urbanski, S., Valentini, R., van der Molen, M., van Gorsel, E., van Huissteden, K., Varlagin, A., Verfaillie, J., Vesala, T., Vincke, C., Vitale, D., Vygodskaya, N., Walker, J.P., Walter-Shea, E., Wang, H., Weber, R., Westermann, S., Wille, C., Wofsy, S., Wohlfahrt, G., Wolf, S., Woodgate, W., Li, Yuelin, Zampedri, R., Zhang, J., Zhou, G., Zona, D., Agarwal,, D., Biraud, S., Torn, M., Papale, D., 2020. The FLUXNET2015 dataset and the ONEFlux

processing pipeline for eddy covariance data. Sci. Data 7, 225. https://doi.org/10.1038/s41597-020-0534-3.

Pastorello, G.Z., Papale, D., Chu, H., Trotta, C., Agarwal, D.A., Canfora, E., Baldocchi, D. D., Torn, M.S., 2017. A new data set to keep a sharper eye on land-air exchanges. Eos (Washington DC) 98, 5.

Paul-Limoges, E., Wolf, S., Schneider, F.D., Longo, M., Moorcroft, P., Gharun, M., Damm, A., 2020. Partitioning evapotranspiration with concurrent eddy covariance measurements in a mixed forest. Agric. For. Meteorol. 280, 107786 https://doi.org/10.1016/j.agrformet.2019.107786.

Paulus, S., El-Madany, T.S., Orth, R., Hildebrandt, A., Wutzler, T., Carrara, A., Moreno, G., Perez-Priego, O., Kolle, O., Reichstein, M., Migliavacca, M., 2021. Lysimeter based evaporation and condensation dynamics in a Mediterranean ecosystem. Hydrol. Earth Syst. Sci. Discuss. 1–29. https://doi.org/10.5194/hess-2021-519.

Poyatos, R., Granda, V., Flo, V., Adams, M.A., Adorján, B., Aguadé, D., Aidar, M.P.M., Allen, S., Alvarado-Barrientos, M.S., Anderson-Teixeira, K.J., Aparecido, L.M., Arain, M.A., Aranda, I., Asbjornsen, H., Baxter, R., Beamesderfer, E., Berry, Z.C., Berveiller, D., Blakely, B., Boggs, J., Bohrer, G., Bolstad, P.V., Bonal, D., Bracho, R., Brito, P., Brodeur, J., Casanoves, F., Chave, J., Chen, H., Cisneros, C., Clark, K., Cremonese, E., Dang, H., David, J.S., David, T.S., Delpierre, N., Desai, A.R., Do, F.C., Dohnal, M., Domec, J.-.C., Dzikiti, S., Edgar, C., Eichstaedt, R., El-Madany, T.S., Elbers, J., Eller, C.B., Euskirchen, E.S., Ewers, B., Fonti, P., Forner, A., Forrester, D.I., Freitas, H.C., Galvagno, M., Garcia-Tejera, O., Ghimire, C.P., Gimeno, T.E., Grace, J., Granier, A., Griebel, A., Guangyu, Y., Gush, M.B., Hanson, P.J., Hasselquist, N.J., Heinrich, I., Hernandez-Santana, V., Herrmann, V., Hölttä, T., Holwerda, F., Irvine, J., Isarangkool Na Ayutthaya, S., Jarvis, P.G., Jochheim, H., Joly, C.A., Kaplick, J., Kim, H.S., Klemedtsson, L., Kropp, H., Lagergren, F., Lane, P., Lang, P., Lapenas, A., Lechuga, V., Lee, M., Leuschner, C., Limousin, J.-.M., Linares, J.C., Linderson, M.-.L., Lindroth, A., Llorens, P., López-Bernal, Á., Loranty, M.M., Lüttschwager, D., Macinnis-Ng, C., Maréchaux, I., Martin, T.A., Matheny, A., McDowell, N., McMahon, S., Meir, P., Mészáros, I., Migliavacca, M., Mitchell, P., Mölder, M., Montagnani, L., Moore, G.W., Nakada, R., Niu, F., Nolan, R.H., Norby, R., Novick, K., Oberhuber, W., Obojes, N., Oishi, A.C., Oliveira, R.S., Oren, R., Ourcival, J.-.M., Paljakka, T., Perez-Priego, O., Peri, P.L., Peters, R.L., Pfautsch, S., Pockman, W.T., Preisler, Y., Rascher, K., Robinson, G., Rocha, H., Rocheteau, A., Röll, A., Rosado, B.H.P., Rowland, L., Rubtsov, A.V., Sabaté, S., Salmon, Y., Salomón, R.L., Sánchez-Costa, E., Schäfer, K.V.R., Schuldt, B., Shashkin, A., Stahl, C., Stojanović, M., Suárez, J.C., Sun, G., Szatniewska, J., Tatarinov, F., Tesař, M., Thomas, F.M., Tor-ngern, P., Urban, J., Valladares, F., van der Tol, C., van Meerveld, I., Varlagin, A., Voigt, H., Warren, J., Werner, C., Werner, W., Wieser, G., Wingate, L., Wullschleger, S., Yi, K., Zweifel, R., Steppe, K., Mencuccini, M., Martínez-Vilalta, J., 2021. Global transpiration data from sap flow measurements: the SAPFLUXNET database. Earth Syst. Sci. Data 13, 2607–2649. https://doi.org/10.5194/essd-13-2607-2021.

Poyatos, R., Granda, V., Molowny-Horas, R., Mencuccini, M., Steppe, K., Martínez-Vilalta, J., 2016. SAPFLUXNET: towards a global database of sap flow measurements. Tree Physiol. 36, 1449–1455. https://doi.org/10.1093/treephys/tpw110.

Reichstein, M., Falge, E., Baldocchi, D., Papale, D., Aubinet, M., Berbigier, P., Bernhofer, C., Buchmann, N., Gilmanov, T., Granier, A., Grünwald, T., Havránková, K., Ilvesniemi, H., Janous, D., Knohl, A., Laurila, T., Lohila, A., Loustau, D., Matteucci, G., Meyers, T., Miglietta, F., Ourcival, J.-.M., Pumpanen, J., Rambal, S., Rotenberg, E., Sanz, M., Tenhunen, J., Seufert, G., Vaccari, F., Vesala, T., Yakir, D., Valentini, R., 2005. On the separation of net ecosystem exchange into assimilation and ecosystem respiration: review and improved algorithm. Glob. Chang. Biol. 11, 1424–1439. https://doi.org/10.1111/j.1365-2486.2005.001002.x.

Roo, F.D., Zhang, S., Huq, S., Mauder, M., 2018. A semi-empirical model of the energy balance closure in the surface layer. PLoS One 13, e0209022. https://doi.org/10.1371/journal.pone.0209022.

Scott, R.L., Knowles, J.F., Nelson, J.A., Gentine, P., Li, X., Barron-Gafford, G., Bryant, R., Biederman, J.A., 2021. Water availability impacts on evapotranspiration partitioning. Agric. For. Meteorol. 297, 108251 https://doi.org/10.1016/j.agrformet.2020.108251.

Stoy, P.C., El-Madany, T.S., Fisher, J.B., Gentine, P., Gerken, T., Good, S.P., Klosterhalfen, A., Liu, S., Miralles, D.G., Perez-Priego, O., Rigden, A.J., Skaggs, T.H., Wohlfahrt, G., Anderson, R.G., Coenders-Gerrits, A.M.J., Jung, M., Maes, W.H., Mammarella, I., Mauder, M., Migliavacca, M., Nelson, J.A., Poyatos, R.,

Reichstein, M., Scott, R.L., Wolf, S., 2019. Reviews and syntheses: turning the challenges of partitioning ecosystem evaporation and transpiration into opportunities. Biogeosciences 16, 3747–3775. https://doi.org/10.5194/bg-16-3747-2019.

Stoy, P.C., Mauder, M., Foken, T., Marcolla, B., Boegh, E., Ibrom, A., Arain, M.A., Arneth, A., Aurela, M., Bernhofer, C., Cescatti, A., Dellwik, E., Duce, P., Gianelle, D., van Gorsel, E., Kiely, G., Knohl, A., Margolis, H., McCaughey, H., Merbold, L., Montagnani, L., Papale, D., Reichstein, M., Saunders, M., Serrano-Ortiz, P., Sottocornola, M., Spano, D., Vaccari, F., Varlagin, A., 2013. A data-driven analysis of energy balance closure across FLUXNET research sites: the role of landscape scale heterogeneity. Agric. For. Meteorol. 171–172, 137–152. https://doi.org/10.1016/j.agrformet.2012.11.004.

Stull, R.B., 1988. An Introduction to Boundary Layer Meteorology. Springer Science & Business Media.

Sun, X., Wilcox, B.P., Zou, C.B., 2019. Evapotranspiration partitioning in dryland ecosystems: a global meta-analysis of in situ studies. J. Hydrol. (Amst.) 576, 123–136. https://doi.org/10.1016/j.jhydrol.2019.06.022.

van Dijk, A.I.J.M., Gash, J.H., van Gorsel, E., Blanken, P.D., Cescatti, A., Emmel, C., Gielen, B., Harman, I.N., Kiely, G., Merbold, L., Montagnani, L., Moors, E., Sottocornola, M., Varlagin, A., Williams, C.A., Wohlfahrt, G., 2015. Rainfall interception and the coupled surface water and energy balance. Agric. For. Meteorol. 214–215, 402–415. https://doi.org/10.1016/j.agrformet.2015.09.006.

Wartenburger, R., Seneviratne, S.I., Hirschi, M., Chang, J., Ciais, P., Deryng, D., Elliott, J., Folberth, C., Gosling, S.N., Gudmundsson, L., Henrot, A.-.J., Hickler, T., Ito, A., Khabarov, N., Kim, H., Leng, G., Liu, J., Liu, X., Masaki, Y., Morfopoulos, C., Müller, C., Schmied, H.M., Nishina, K., Orth, R., Pokhrel, Y., Pugh, T.A.M., Satoh, Y., Schaphoff, S., Schmid, E., Sheffield, J., Stacke, T., Steinkamp, J., Tang, Q., Thiery, W., Wada, Y., Wang, X., Weedon, G.P., Yang, H., Zhou, T., 2018. Evapotranspiration simulations in ISIMIP2a—Evaluation of spatio-temporal characteristics with a comprehensive ensemble of independent datasets. Environ. Res. Lett. 13, 075001 https://doi.org/10.1088/1748-9326/aac4bb.

Wehr, R., Commane, R., Munger, J.W., McManus, J.B., Nelson, D.D., Zahniser, M.S., Saleska, S.R., Wofsy, S.C., 2017. Dynamics of canopy stomatal conductance, transpiration, and evaporation in a temperate deciduous forest, validated by carbonyl sulfide uptake. Biogeosciences 14, 389–401. https://doi.org/10.5194/bg-14-389-2017.

Wilson, K., Goldstein, A., Falge, E., Aubinet, M., Baldocchi, D., Berbigier, P., Bernhofer, C., Ceulemans, R., Dolman, H., Field, C., Grelle, A., Ibrom, A., Law, B.E., Kowalski, A., Meyers, T., Moncrieff, J., Monson, R., Oechel, W., Tenhunen, J., Valentini, R., Verma, S., 2002. Energy balance closure at FLUXNET sites. Agric. For. Meteorol. 113, 223–243. https://doi.org/10.1016/S0168-1923(02)00109-0.

Wohlfahrt, G., Widmoser, P., 2013. Can an energy balance model provide additional constraints on how to close the energy imbalance? Agric. For. Meteorol. 169, 85–91. https://doi.org/10.1016/j.agrformet.2012.10.006.

Xiao, W., Wei, Z., Wen, X., 2018. Evapotranspiration partitioning at the ecosystem scale using the stable isotope method—A review. Agric. For. Meteorol. 263, 346–361. https://doi.org/10.1016/j.agrformet.2018.09.005.

Xu, T., Guo, Z., Liu, S., He, X., Meng, Y., Xu, Z., Xia, Y., Xiao, J., Zhang, Y., Ma, Y., Song, L., 2018. Evaluating different machine learning methods for upscaling evapotranspiration from flux towers to the regional scale. J. Geophys. Res. 123, 8674–8690. https://doi.org/10.1029/2018JD028447.

Zhang, K., Zhu, G., Ma, J., Yang, Y., Shang, S., Gu, C., 2019. Parameter Analysis and Estimates for the MODIS evapotranspiration algorithm and multiscale verification. Water Resour. Res. 55, 2211–2231. https://doi.org/10.1029/2018WR023485.

Zhang, W.J., 2022. WJ714/HRHC_mpi_bgc: Weijie_Zhang_HighRelativeHumidityCorrection (v-1.0). Zenodo. https://doi.org/10.5281/zenodo.7083230.

Zhang, Y., Peña-Arancibia, J.L., McVicar, T.R., Chiew, F.H.S., Liu, C., Lu, X., Zheng, H., Wang, Y., Liu, Y.Y., Miralles, D.G., Pan, M., 2016. Multi-decadal trends in global terrestrial evapotranspiration and its components. Sci. Rep. 6, 19124. https://doi.org/10.1038/srep19124.

Zhou, S., Yu, B., Zhang, Y., Huang, Y., Wang, G., 2016. Partitioning evapotranspiration based on the concept of underlying water use efficiency: ET partitioning. Water Resour. Res. 52, 1160–1175. https://doi.org/10.1002/2015WR017766.

Zhou, Y., Li, D., Liu, H., Li, X., 2018. Diurnal variations of the flux imbalance over homogeneous and heterogeneous landscapes. Bound.-Layer Meteorol. 168, 417–442. https://doi.org/10.1007/s10546-018-0358-2.